ISSN (Print) : 2337-9030 ISSN (Online) : 2685-2608
PILLAR OF PHYSICS
JURNAL BERKALA ILMIAH FISIKA
Vol. 19 (1), 2026, page. 18-26
DOI: https://doi.org/10.24036/89zdna282

IDENTIFICATION OF LIQUEFACTION POTENTIAL IN KOTO TANGAH SUBDISTRICT OF PADANG CITY USING SCHLUMBERGER CONFIGURATION GEOELECTRIC METHOD

Nelma Yeti[1*], Akmam[1], Hamdi[1], Nofi Yendri Sudiar[1]

[1]*Department of Physics, Universitas Negeri Padang, Jl. Prof. Dr. Hamka Air Tawar Padang 25131, Indonesia*
Corresponding author. Email: akmam_db@fmipa.unp.ac.id

ABSTRACT

The earthquake of September 30 2009, showed that Lubuk Buaya Sub-district, Koto Tangah Sub-district, Padang City is an earthquake-prone area, and the geology of the area consisting of sandstone and alluvium deposits is a contributing factor to liquefaction. Research on liquefaction potential using the Schlumberger configuration geoelectric method has never been conducted in this area, although initial observations showed indications of liquefaction in buildings and infrastructure. Therefore, this study aims to determine the description of soil layers that have the potential to experience liquefaction based on the value of rock specific resistance in Lubuk Buaya Village. This research used a descriptive field approach, conducted from February to June 2025 with four measurement tracks, each 155 meters long and 5 meters electrode spacing. Using the Automatic Resistivity System (ARES) instrument with power up to 850 W and current up to 5.0 A. The data obtained include electric current strength (I), potential difference (V), and electrode spacing which are processed to determine the value of geometry factor and apparent density resistance (ρa). Data interpretation was carried out using the Smoothness Constraint Least Squares inversion method with the help of Res2dinv software to produce true specific resistivity and depth. The results showed that the subsurface soil layers in Lubuk Buaya Village have a high potential to experience liquefaction. This potentially liquefiable soil layer consists of water-saturated sand, gravel, and sandy silt, with low resistivity values. Liquefaction potential zones were identified at depths of 5 to 25 meters with a thickness of 20 meters.

Keywords: *Liquefaction, Geoelectric, Schlumberger, Koto Tangah, Resistivity*

I. INTRODUCTION

Geographically, Padang City is located on the west coast of Sumatra Island and has a high earthquake hazard vulnerability. This is due to the presence of the Sumatra subduction zone to the west of Padang City which moves around 40 to 70 mm/year [1] [14]. Earthquakes can trigger liquefaction phenomena, especially in areas with loose and water-saturated soil structures, as was the case with the September 30 2009 earthquake that caused significant damage in Koto Tangah Subdistrict [20].

The Atlas of Indonesian Liquefaction Vulnerability Zones released by the Ministry of Energy and Mineral Resources [7], states that the Lubuk Buaya Village area in Koto Tangah Subdistrict, which is included in the Padang City, is in a moderate liquefaction vulnerability zone, which is a vulnerability zone that can experience liquefaction unevenly and the soil structure is generally damaged [8]. Seismic activity is also a determining factor for liquefaction susceptibility, where this event depends on the intensity of the earthquake. Based on the results of research [16], Lubuk Buaya Village has a high seismic vulnerability index. Initial observations on March 10, 2025 showed that several houses experienced subsidence, cracks in the walls and foundations, and cracks in the river embankment. Buildings at coordinates 0°49'22“ S and 100°19'00” E had 2-3 cm wall cracks, while buildings at 0°49'07" E and 100°19'22" S experienced foundation settlement. The river embankment at 0°49'26 “S and 100°19'2 ”E experienced 2-3 cm cracks, and the natural marshland at 0°49'28“ E and 100°19'22” S experienced foundation settlement 100°18'54" S showed instability when stepped on, with the ground surface

Submitted: 03-08-2025 Accepted: 30-04-2026 Published: 30-04-2026

swaying like waves. This incident has raised concerns among the public about the safety of their homes and the long-term impact of this phenomenon.

Liquefaction is a change in soil condition from solid to liquid. Liquefaction is often found in earthquake events where soil behavior occurs due to earthquake loads that occur only in a short time [10]. Liquefaction only occurs in saturated soils, so the depth of the water table will affect the potential for liquefaction [12]. Apparent resistivity values are influenced by rock density, porocity, and water content. Liquefaction can only occur under certain conditions, if a soil does not meet these conditions, then the soil does not have the potential for liquefaction. Therefore, development planning should avoid soils that have met the conditions for liquefaction [9]. The conditions for liquefaction include the presence of water-saturated soil layers, soil layers in the form of silt or sand, loose (not solid), and an earthquake with a magnitude above 5,0.

Liquefaction can be detected using the Geoelectric method, the basic principle of the Geoelectric method is to measure the electrical resistance of the earth's subsurface layer through measuring the potential difference generated by an electric current injected into the earth's surface and measuring the potential difference generated at the earth's surface. The specific gravity obtained from the Geoelectric method measurement is a pseudo specific gravity, assuming the earth as a homogeneous and isotropic medium [3]. The earth is assumed to be an isotropic homogeneous medium in reality is a nonhomogeneous medium, so the measured value of the specific gravity is not the actual specific gravity value but the apparent specific gravity value. The apparent density resistance value is formulated as follows:

$$\rho_a = K\frac{\Delta V}{I} \qquad (1)$$

Where ρ_a is the apparent density resistance value, K is the geometry factor value, ΔV is the potential difference and I is the current value. The value of K depends on the type of configuration used. The configuration used in this research is the Schlumberger Configuration Geoelectric method. The Schlumberger configuration uses four electrodes with two potential electrodes and two current electrodes arranged in a straight line with the arrangement of the potential electrode distance smaller than the current electrode distance [21]. The advantage of the Schlumberger configuration is its ability to detect the inhomogeneous nature of rock layers at the surface. The Schlumberger arrangement is also used for mapping or profiling lateral resistivity changes [2]. Compared to Wenner, Schlumberger is more effective at determining vertical (depth) resistivity changes efficiently, making it theprimary choice for drilled well surveys. The electrode array of the Schlumberger configuration is shown in Figure 1.

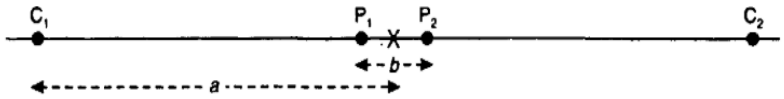

Fig. 1. Schlumberger Configuration Electrode Arrangement

Figure 1 shows that electrodes P1 and P2 are used as potential electrodes and electrodes C_1 and C_2 are used as current electrodes with a distance on each electrode. The geometry factor of the Schlumberger configuration can be calculated using the formula: [6]

$$K = \pi\frac{L^2}{4l}\left[I - \frac{l^2}{L^2}\right] \qquad (2)$$

Where L is the current electrode distance (A), l is the potential electrode distance (V). The depth that can be measured using the Schlumberger configuration geoelectric method is 1/5 of the current electrode distance C_1, C_2 used. The apparent specific gravity value obtained from the measurement can be interpreted using an inversion method to produce the true specific gravity value and depth [5]. The inversion method generally does not produce unique information, so it is necessary to add some additional information. This additional information is used to constrain a solution [18], so that accurate information can be obtained about objects under the earth's surface. There are several types of 2D inversion methods, and the one used in this study is Smoothness-Constraint Least Squares Inversion. This method is an inversion method that tends to produce a model with smooth variations in resistivity values [2]. Smoothness-Constraint Least Squares inversion is formulated with the following equation:

$$(J^TJ + \lambda F)d = J^Tg - \lambda Fr \qquad (3)$$

Where F is $f_x{f_x}^T + f_Z{f_z}^T$, f_x is the horizontal flatness filter, f_Z is the vertical flatness filter, J is the partial derivative matrix, λ is the damping factor, d is the perturbation vector of the model, g is the discrepancy vector, and r is a vector containing the logarithm of the model resistivity value [6]. The advantage of this method is that

in addition to producing a smooth resistivity value, the damping factor and filter can be adjusted to various types of data. Damping factor is a variable related to the process of dampening instability that may arise due to data limitations in the inversion. Damping factor is determined by trial and error. To minimize the error, a small value of damping factor can be used.

II. METHOD

This research uses a descriptive approach to provide a detailed description of the object under study based on data collected directly at the research location. The research location is located in Koto Tangah, precisely in Lubuk Buaya Village. The research procedure is divided into 3 stages, namely:

1. Preparatory Stage

The preparatory stage begins with a theoretical study of the theories that support the research. Then conduct a preliminary survey to the research area to determine the length of the track and the electrode spacing that will be used during the measurement. Then prepare the material tools needed before conducting research. In the preparation stage, 4 research trajectories were designed. The measurement track design can be seen in Figure 2.

Fig. 2. Research Trajectory Map

Figure 2 is the measurement trajectory design. Point A marks the starting point (location of the first electrode) with coordinates 0°49'27" S and 100°18'54" E and A' marks the end point (the location of the last electrode) with coordinates 0°49'24" S and 100°18'53" E of the first track, point B marks the starting point (location of the first electrode) with coordinates 0°49'23" S and 100°18'53" E and B' marks the end point (location of the last electrode) with coordinates 0°49'21" S and 100°18'57" E of the second traverse, point C marks the starting point (location of the first electrode) with coordinates 0°49'26" S and 100°18'54" E and C' marks the end point (location of the last electrode) with coordinates 0°49'24" S and 100°18'58" E of the third track, and point D marks the starting point (location of the first electrode) with coordinates 0°49'28" S and 100°18'54" E and D' marks the end point (location of the last electrode) with coordinates 0°49'26" S and 100°18'59" E of the fourth trajectory.

2. Data Collection Phase

Data collection is carried out by preparing a measurement trajectory in the form of a straight line according to the depth to be achieved. Measuring the length of the track and electrode spacing, then planting electrodes at each spacing. The current source and cable connection to the electrode were checked and the electrode cable was connected to the current source. Next, ARES was activated and it was confirmed that the battery was 85%

charged. After that, the ARES tool was calibrated and the measurement method and configuration were selected, and then the measurement was carried out.

3. Data Analysis Technique

Measurement data in the form of electric current strength (I), potential difference (V), and electrode spacing will be stored in the ARES main unit, then the stored data is downloaded. To determine the value of the geometry factor can be calculated by equation (2), and the apparent density resistance value by equation (1). Because the amount of data obtained is a lot, Microsoft Excel assistance is used. The apparent specific resistivity value obtained is interpreted using the inversion method to produce the true specific resistivity and depth [6]. The inversion method used is Smoothness - Constraint Least Squares. The inversion process can be done using equation (3). Given the large amount of data used, to simplify and speed up the inversion process, Res2dinv software is used. The use of this software allows for more efficient and accurate data processing. Data interpretation produces the actual value of specific gravity and depth, in the form of 2D cross-section of the earth's subsurface. The actual value of specific gravity in the 2D cross-section model is estimated using the value of rock specific gravity [19], the geological conditions of the research area, and the observation of dug wells owned by residents around the research location.

III. RESULTS AND DISCUSSION

A. Results

The following are the measurement and interpretation results for each track:

1. Track 1

Measurement of track 1 starts from the coordinates 0°49'28" S and 100°18'54" E to the north with coordinates 0°49'23" S and 100°18'52" E. The sounding point of Track 1 is at coordinates 0°49'26" S and 100°18'54" E.

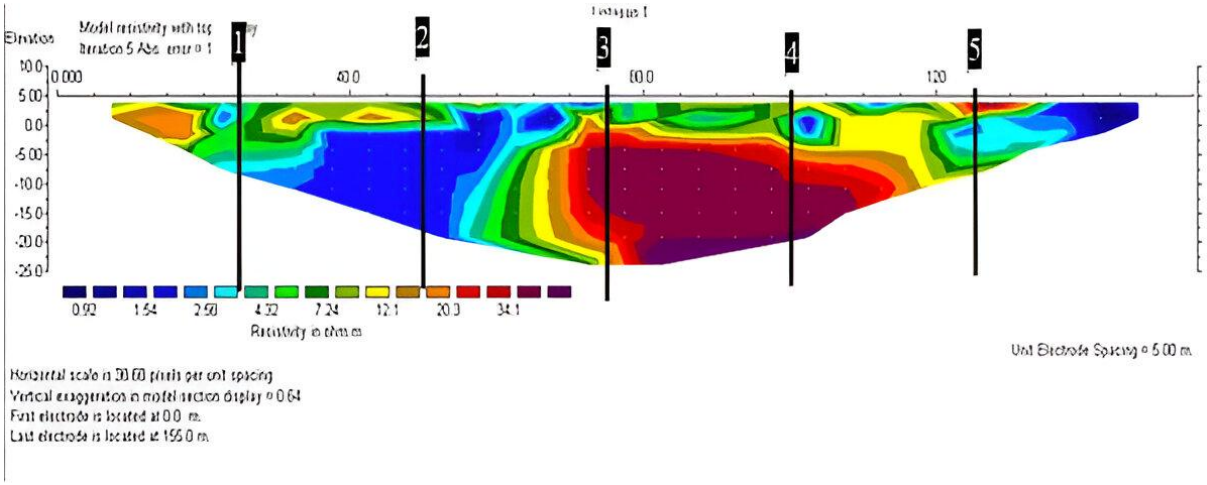

Fig. 3. Cross-section of 2D Model of Specific Resistivity of Trajectory 1

The Cross-section of 2D Model of Specific Resistivity of Trajectory 1 in figure 3 shows a percentage error obtained at the fifth iteration of 10.5%. The maximum depth that can be detected is 31 meters. The distribution of the specific resistivity value of Track 1 ranges from 0.92 - >34.1 Ωm.

2. Track 2

Measurement of track 2 starts from coordinates 0°49'23" S and 100°18'53" E towards the East with coordinates 0°49'22" S and 100°18'57" E. The sounding point of track 2 is at coordinates 0°49'22.18" S and 100°18'55.04" E.

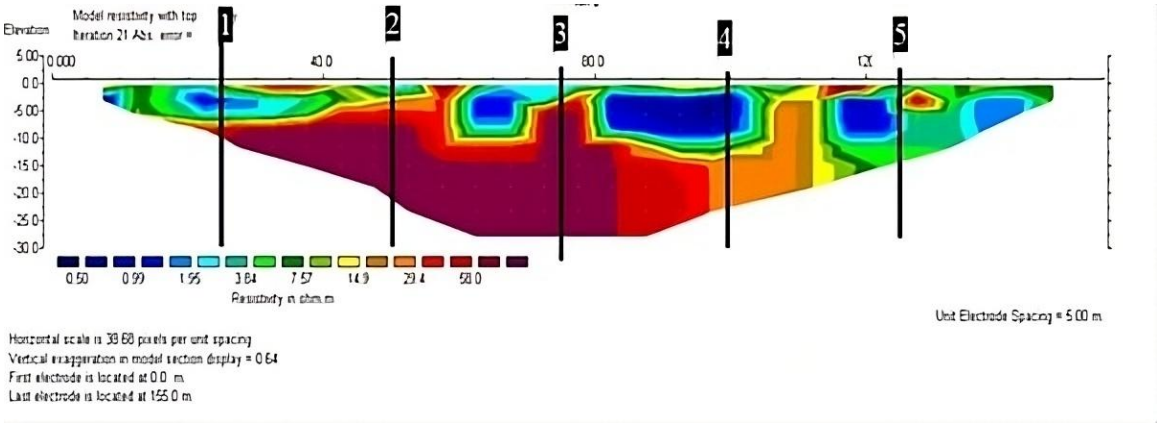

Fig. 4. Cross section of 2D Model of Specific Resistivity of Trajectory 2

Figure 4 shows the cross-section of the 2D model of the specific gravity of Trajectory 2 with a percentage error obtained at the 21st iteration of 14.9%. The maximum depth that can be detected is 31 meters. The distribution of the specific resistivity value of Track 2 ranges from 0.50 - 58.0 Ωm.

3. Trajectory 3

Measurement of track 3 starts from coordinates 0°49'26.4" S and 100°18'53" E towards the East with coordinates 0°49'24" S and 100°18'58" E. The sounding point is located at coordinates 0°49'25" S and 100°18'56" E.

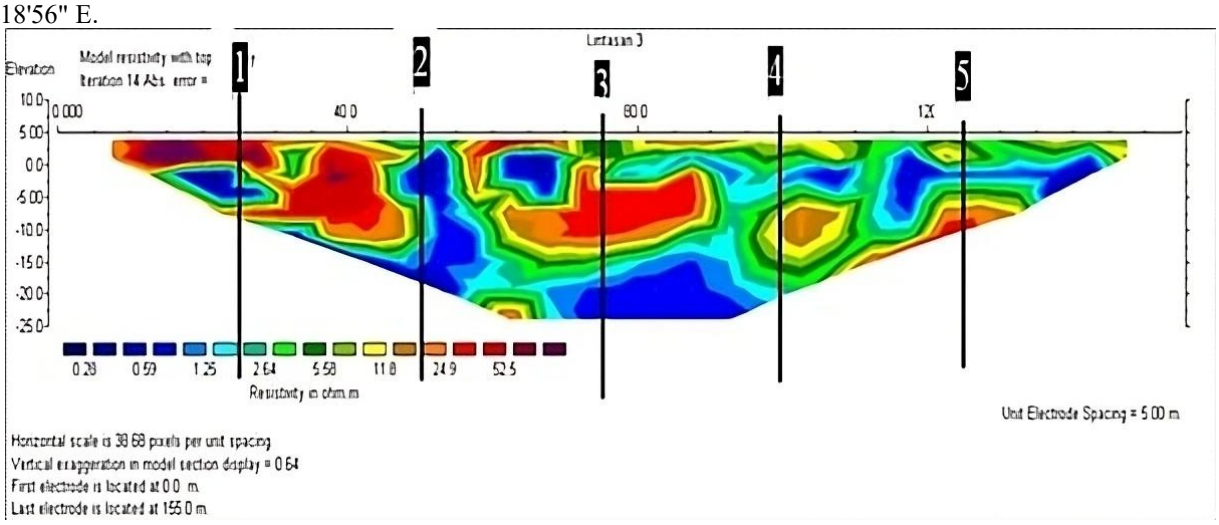

Fig. 5. Cross-section of 2D Model of Specific Resistivity of Trajectory 3

The cross-section of the 2D model of specific gravity of Trajectory 3 in figure 5 shows a percentage error obtained at the 14th iteration of 10.8%. The distribution of the specific resistivity value of Trajectory 3 ranges from 0.28 - >52.5 Ωm. With depth penetration reaching 31 meters.

4. Trajectory 4

The measurement of track 4 starts from the coordinates 0°49'28" S and 100°18'54" E to 0°49'25" S and 100°18'59" E. The measurement sounding point is at coordinates 0°49'27" S and 100°18'56" E.

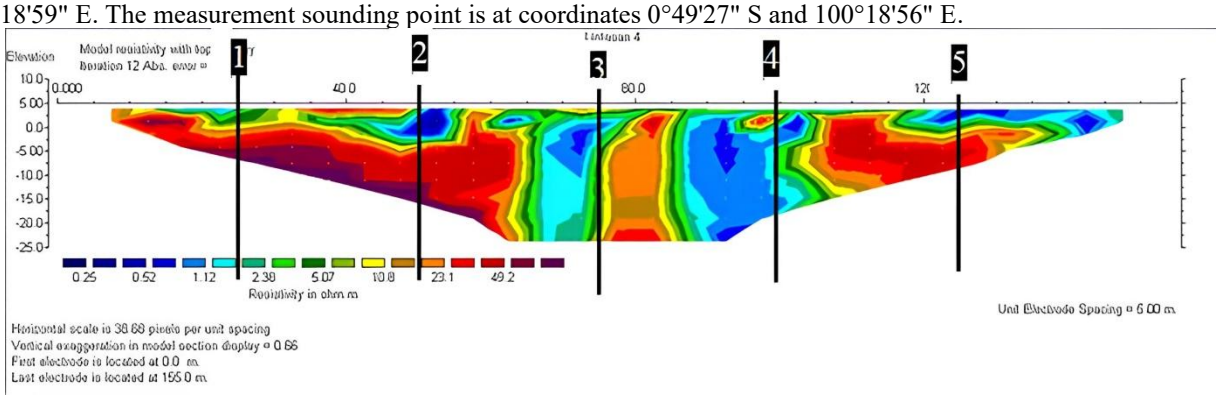

Fig. 6. Cross-section of 2D Model of Specific Resistivity of Trajectory 4

Figure 6 shows a cross-section of the 2D model of the specific gravity of Trajectory 4 with a percentage error obtained at the 12th iteration of 12.5%. The maximum depth that can be detected is 31 meters. The distribution of the specific resistivity value of Trajectory 3 ranges from 0.25 - 49.2 Ωm.

B. Interpretative Discussion

The data from track 1 shows a varied subsurface resistivity distribution with a percentage measurement error of 10.5%, the 2D model cross section of the specific gravity of Track 1 is estimated to contain 3 types of rocks, namely sand and gravel containing brackish water, sandy silt, sandy silt and gravel. Along 25 meters there is estimated to be sandy silt rock with a thickness of 12.5 meters. Along 50 meters there are sand and gravel rocks with a thickness of 17.5 meters, and sandy silt with a thickness of 4 meters. The low resistivity value in this layer indicates the presence of brackish water content [11]. Along 75 meters there are sandy silt rocks with a thickness of 7.5 meters and sandy silt and gravel with a thickness of 22.5 meters. Along 100 meters, it is estimated that there are sandy silt rocks with a thickness of 12.5 meters, sandy silt and gravel with a thickness of 11.5 meters. Along 125 meters it is estimated that there are sand and gravel rocks with a thickness of 6 meters, sandy silt 5 meters and silt sand and gravel 5 meters.

Soil deposits that have a lot of liquefaction are fine sand, silty sand, muddy sand and ordinary sand with a resistivity value of around 10 Ωm to 100 Ωm [10]. The liquefaction potential zone of track 1 is estimated at measuring points 40 meters to 65 meters, composed of sand and gravel rocks with a thickness of 20 meters. This is in accordance with the geological conditions of the study area, namely alluvial deposits composed of sand, silt and gravel [20]. This layer is indicated to contain brackish water so that it becomes a water-saturated zone [15]. Under water-saturated and loose conditions, soil grains do not have strong intergranular contact, so that during seismic shaking, pore water pressure increases dramatically beyond the effective stress of the soil, causing the soil to lose shear strength and behave like a liquid [16]. The water stored in this saturated zone is brackish water that has been mixed with sand and gravel with a resistivity of 0.92 - 2.98 Ωm. The depth of the water table at this location ranges from 1 m to 20 m. Therefore, the very low resistivity in the area is a strong indicator of water accumulation and unstable soil types against dynamic loads such as earthquakes. These two things make this layer a zone that has the potential to experience liquefaction in the event of a large earthquake. On this track, indications of liquefaction can be seen from cracks in the river embankment with coordinates 0°49'26" S and 100°19'2" E.

The data from track 2 shows a varied subsurface resistivity distribution with a measurement error percentage of 14.9%, the 2D model cross section of the specific gravity of Track 2 is estimated to contain 3 types of rocks, namely sand and gravel containing brackish water, sandy silt, sandy silt and gravel. Along 25 meters there are estimated to be sand and gravel rocks with a thickness of 3 meters, sandy silt 2 meters and silt sand and gravel 2 meters. Along 50 meters, sandy silt is estimated to be 4 meters thick, sandy silt and gravel 18.5 meters. Along 75 meters it is estimated that there are sand and gravel rocks with a thickness of 2 meters, sandy silt 1 meter and sandy silt and gravel 25 meters. Along 100 meters it is estimated that there are sand and gravel rocks with a thickness of 8 meters, sandy silt 3.5 meters, sandy silt and gravel 10 meters. Along 125 meters it is estimated that there are sand and gravel rocks with a thickness of 1 meter, sandy silt 5 meters and 9 meters.

The potential liquefaction zone of track 2 is estimated to be at measurement points 65 meters to 100 meters, composed of sand and gravel rocks with a thickness of 10 meters. This is in accordance with the geological conditions of the study area, namely alluvial deposits composed of sand, silt and gravel [20]. This layer is indicated to contain brackish water so that it becomes a water-saturated zone [15]. The water stored in this saturated zone is brackish water that has been mixed with sand and gravel with a resistivity of 0.50 - 1.96 Ωm. The constituent materials of this layer are silt and sand which are the geological conditions most susceptible to liquefaction, very low resistivity in the area is a strong indicator of water accumulation and unstable soil types against dynamic loads such as earthquakes. The depth of the water table at this location ranges from 1 m to 10 m, indicating that this trajectory has the potential for liquefaction.

In the data from track 3 shows a varied subsurface resistivity distribution with a percentage measurement error of 10.8%, the cross section of the 2D model of specific gravity of Track 3 is estimated to have 3 types of rocks, namely sand and gravel containing brackish water, sandy silt, sandy silt and gravel [17]. Along 25 meters there are estimated to be sand and gravel rocks with a thickness of 4 meters, sandy silt 7 meters and silt sand and gravel 3 meters. Along 50 meters it is estimated that there are sand and gravel rocks with a thickness of 7 meters, sandy silt 8 meters. Along 75 meters it is estimated that there are sand and gravel rocks with a thickness of 7 meters, sandy silt 8 meters and sandy silt and gravel 8 meters. Along 100 meters, sand and gravel with a thickness of 2.5 meters, sandy silt 7.5 and 18.5 meters are estimated. Along 125 meters it is estimated that there are sand and gravel rocks with a thickness of 2.5 meters, sandy silt 5 meters and silty sand and gravel 2.5 meters. This is in accordance with the geological conditions of the study area, namely alluvial deposits composed of sand, silt and gravel [20].

The liquefaction potential zone of track 3 is estimated to be at measurement points 50 meters to 90 meters, composed of sandstone and gravel with a thickness of 23 meters. This layer is indicated to contain

brackish water, making it a water-saturated zone [15]. The saturated zone containing brackish water, mixed with sand and gravel rocks that have resistivity between 0.28 to 1.25 Ωm, shows significant liquefaction potential. This is due to the high water content in the soil, which causes the water pressure in the pores to increase, especially during vibration. Soil structures consisting of sand and gravel, which tend to be uncompacted, can lose their shear strength when exposed to vibration, thus behaving like a liquid. In addition, the depth of the water table, which ranges from 1 m to 23 m, indicates that the overlying soil layers may not be stable enough to withstand the pressure from the underlying layers. When external vibrations occur, such as earthquakes or construction activities, the water pressure in the soil pores may increase, causing the soil to lose cohesion and increasing the risk of liquefaction [12], considering all these factors, the site has conditions that favor liquefaction, especially in situations of significant shaking or loading.

In the data from track 4 results show a varied subsurface resistivity distribution with a percentage measurement error of 12.5%, the 2D model cross section of the specific gravity of Track 4 is estimated to have 3 types of rocks, namely sand and gravel containing salt water, sandy silt, sandy silt and gravel. Along 25 meters there are estimated to be sandy silt rocks with a thickness of 7 meters and silt sand and gravel of 6.5 meters. Along 50 meters there are sand and gravel rocks with a thickness of 8 meters, sandy silt 4 meters, sand silt and gravel 8 meters. Along 75 meters it is estimated that there are sand and gravel rocks with a thickness of 7.5 meters, and sandy silt 2.5 meters and 20 meters. Along 100 meters it is estimated that there are sand and gravel rocks with a thickness of 3 meters and 5 meters, sandy silt 5 and 9.5 meters. Along 125 meters it is estimated that there are sand and gravel rocks with a thickness of 3 meters, sandy silt 4.5 meters, silt sand and gravel 6.5 meters.

The liquefaction potential zone of track 4 is estimated to be at measurement points 70 meters to 90 meters, composed of sandstone and gravel with a thickness of 22 meters. This layer is indicated to contain brackish water, making it a water-saturated zone [15]. The saturated zone containing brackish water, mixed with sand and gravel rocks that have resistivity between 0.25 to 2.38 Ωm, shows significant liquefaction potential. This is due to the high water content in the soil, which causes the water pressure in the pores to increase, especially during vibration. Soil structures consisting of sand and gravel, which tend to be uncompacted, can lose their shear strength when exposed to vibration, thus behaving like a liquid. In addition, the depth of the water table, which ranges from 1 m to 23 m, indicates that the overlying soil layers may not be stable enough to withstand the pressure from the underlying layers [8]. When external vibrations occur, such as earthquakes or construction activities, the water pressure in the soil pores may increase, causing the soil to lose cohesion and increasing the risk of liquefaction, taking all these factors into account, the site has conditions that favor liquefaction, especially in situations of significant shaking or loading.

The results of the interpretation of liquefaction potential in Lubuk Buaya urban village, Koto Tangah sub-district, identified that this research area has the potential to experience liquefaction, as evidenced by the results of the study which showed the presence of water-saturated soil layers with low resistivity at shallow depths. This is also reinforced by the discovery of several houses that have experienced liquefaction characteristics such as falling foundations and cracked buildings. Geoelectric data obtained indicates that the sand, gravel and sandy silt layers located in the subsurface have characteristics that support liquefaction when vibrations occur, such as those produced by an earthquake. The results of this current research are in line with the results off research [20] whichshows that the subsurface layer consists of water saturated alluvial deposits, which have the potential to experience liquefaction when ann earthquake occurs. Based on the estimation that has been carried out, it is found that the research area has considerable liquefaction potential.

IV. CONCLUSION

This study successfully identified the potential for liquefaction in Lubuk Buaya urban village, Koto Tangah sub-district, based on the rock specific resistivity value of the Schlumberger configuration geoelectric method. The subsurface soil layers in Lubuk Buaya subdistrict show a potential for liquefaction with the dominating soil layers being water-saturated sand, gravel, and sandy silt, with low resistivity values, especially in the depth range of 5 to 20 meters. This finding is reinforced by field observations of structural damage such as foundation settlement and building cracks, which are indicators of liquefaction. Therefore, it can be concluded that the study area is susceptible to liquefaction, especially during an earthquake.

V. ACKNOWLEDGMENT

Thank you, Mr. Lurah Kelurahan Lubuk Buaya, for giving permission and assistance to conduct research. The community and Mr. RT 01, RT 02, RT 03 Abu Hanif Housing Complex block 4A. The Physics Laboratory for accommodating and providing assistance during the research. Thank you also to the Geoelectric team for helping the research implementation.

VI. REFERENCES

[1] Akmam. (2016). Subduksi Lempeng Indo-Australia Pada Lempeng Eurasia di Pantai Barat Sumatera Barat. *Jurnal Sainstek IAIN Batusangkar, 3(1), 52–5*.

[2] Akmam, A., Amir, H., & Putra, A. (2020). Implementation of robust constraint inversion method on resistivity geoelectric data to study landslide precursors (case study : Sungai Lasi District and Gunung Talang Solok District, West Sumatra). *Journal of Physics: Conference Series, 1481(1).*

[3] Akmam, A., Irefia, R. D., Silvia, D., & Jemmy, R. (2015). Optimition Of Least Squares Methods Smooth Constrain Using Occam ' S Inversion Geoelectric Resistivity Dipole-Dipole Consfiguration For Estimation Slip Surface. *In ICOMSET, 154–161, 154–161.*

[4] Akmam, Amir, H., & Putra, A. (2021). Identification Of The Slips Surfaces Using Resistivity Geoelectrical Method In Landslide Prone Areas In Padang And Agam Regency Of West Sumatera. *In Talenta Conference Series: Science and Technology (ST) (Vol. 2, No. 2, Pp. 152-165).*

[5] Akmam, Amir, H., Putra, A., Anshari, R., & Jalinus, N. (2019). Implementation of least-square constrain inversion method of geoelectrical resistivity data Wenner-Schlumberger for investigation the characteristic of landslide. *Journal of Physics: Conference Series, 1185(1).*

[6] Akmam, & Nofi, Yendri Sudiar. (2013). Analisis Struktur Batuan dengan Metoda Inversi Smoothness-Constrained Least-Squares Data Geolistrik Konfigurasi Schlumberger di Universitas Negeri Padang Kampus Air Tawar. *Prosiding SEMIRATA 2013, 1(1)., 215–220.*

[7] Buana, T. W., Hermawan, W., Rahdiyana, R. N., Wahyudin, R. W., Hasibuan, G., Wiyono, & Sollu, W. P. (2019). Atlas Zona Likuefaksi Indonesia. *In Badan Geologi Kementrian Energi dan Sumber Daya Mineral.*

[8] Diyanah, Prasetyo, Y., & Firdaus, H. S. (2018). Studi Korelasi Kapasitas Akuifer Terhadap Penurunan Muka Tanah Dengan Metode Ps-Insar (Studi Kasus : Kota Semarang). *Jurnal Geodesi Undip, 7(4), 206–214.*

[9] Febriana, R. K. N., Minarto, E., & Tryono, F. Y. (2017). Identifikasi Sebaran Aliran Air Bawah Tanah (Groundwater) dengan Metode Vertical Electrical Sounding (VES) Konfigurasi Schlumberger di Wilayah Cepu, Blora Jawa Tengah. *Jurnal Sains Dan Seni ITS, 6(2), 6–10.*

[10] Hakam, A. (2022). Analisis Praktis Potensi Likuifaksi Referensi Untuk Peneliti dan Praktisi (R. Shafira (ed.); Issue August 2020). *Andalas Press Kampus UNAND-Limau Manis, 25176.*

[11] Kamur, S., Iskandar, A., Awal, S., & Nasarudin. (2024). Analisis Potensi Air Tanah Di Kecamatan Molawe Kabupaten Konawe Utara Menggunakan Geolistrik S-Field Multichanel Metode Wenner. *Jurnal Pendidikan, Sains, Geologi*

[12] Mina, E., Kusuma, R. I., & Sudirman, S. (2018). Analisa Potensi Likuifaksi Berdasarkan Data Spt (Studi Kasusproyek Pembangunan Gedung Baru Untirta Sindang Sari). *Jurnal Fondasi, 7(1), 11–21.*

[13] Moechtar, H., Mulyana, H., & Pratomo, I. (2016). Sedimentologi Dan Stratigrafi Holosen Dataran Pantai Medan - Belawan Sekitarnya, Sumatera Utara. *Jurnal Geologi Kelautan, 5(2), 99–111.*

[14] Natawidjaja, D. H., Sieh, K., Ward, S. N., Cheng, H., Edwards, R. L., Galetzka, J., & Suwargadi, B. W. (2004). Paleogeodetic records of seismic and aseismic subduction from central Sumatran microatolls, Indonesia. *Journal of Geophysical Research: Solid Earth, 109(4), 1–34.*

[15] Pryambodo, D. G., & Sudirman, N. (2019). Identifikasi Likuifaksi Di Kawasan Pesisir Kota Padang Dengan Metoda Geolistrik 2D. *Jurnal Segara, 15(3), 159–168.*

[16] Rosyidi, P. (2020). Analisis Potensi Likuifaksi Tanah Berbasis Teknik Gelombang Seismik (S. P. Permana (ed.); I). *The Phinisi Press Yogyakarta.*

[17] Saaduddin, Sismanto, & Marjiyono. (2015). Pemetaan Indeks Kerentanan Seismik Kota Padang Sumatera Barat Dan Korelasinya Dengan Titik Kerusakan Gempabumi 30. *Seminar Nasional Kebumian Ke-8, October, 459–466.*

[18] Supriyanto. (2007). Analisis Data Geofisika : Memahami Teori Inversi. *Universitas Indonesia.*

[19] Telford, W. M., Geldart, L. P., & Sheriff, R. E. (1990). Applied Geophysics Second Edition. *In Sustainability (Switzerland) (Vol. 11, Issue 1).*

[20] Tohari, A., Syahbana, A. J., Satriyo, N. A., & Soebowo, E. (2019). Karakteristik likuifaksi Tanah Pasiran di Kota Padang Berdasarkan Metode Microtremor. *ResearchGate, July, 978–979.*

[21] Usman, B., Manrulu, R. H., Nurfalaq, A., & Rohayu, E. (2017). Identifikasi Akuifer Air Tanah Kota Palopo Menggunakan Metode Geolistrik Tahanan Jenis Konfigurasi Schlumberger. *Jurnal Fisika FLUX, 14(2), 65.*